Global optimization by Very Fast Simulated Annealing algorithm of the 3D CRS and 3D CDS stack parameters: Application to real data of Potiguar Basin, Brazil

German Garabito (UFRN), Heron Schots (CPGeo) and José Tassini (CPGeo)

Abstract

The common-reflection-surface stack method was introduced to simulate high quality zero-offset stacked data from multi-coverage reflection prestack data, but currently it can be also applied for prestack data regularization, velocity model determination and prestack migration. The 3D common-reflection-surface staking operator depends on eight stacking parameters and its use on any of the listed applications requires determination of these parameters from the multi-coverage prestack data by using an optimization strategy based on coherence measurement of the seismic signal. The initial implementations of the 3D common-reflection-surface stack used grid search techniques for searching those parameters in several steps and the accumulated errors can deteriorate the final results. In this work, we use the global optimization Very Fast Simulated Annealing algorithm to simultaneously search for the eight parameters of the common-reflection-surface operator and the five parameters of the common-diffraction-surface stack operator. We applied the proposed global optimization strategies to 3D real dataset acquired in Potiguar Basin, Brazil, and it is shown that the eight-parameter optimization strategy produces the best results but with a higher computational cost.

Introduction

The 3D Common-Reflection-Surface (CRS) stack method has demonstrated to be more robust and efficient than conventional seismic stacking methods, producing clearer images when applied in real datasets of geologically complex media (Cristini et. al, 2002; Bergler et. al., 2002; Borrini, et. Al., 2005; Müller, 2009).

The zero-offset CRS stack operator is a hyperbolic traveltime approximation for reflection events near to the normal central ray. It depends on eight kinematic CRS attributes or CRS parameters. Those attributes have important applications, such as, velocity model determination by tomographic inversion, prestack migration and data regularization. The main challenge of the CRS stack method is to find a computationally efficient strategy to determine accurately the CRS parameters for each time sample of the stacked trace by automatic search processes based on coherence analysis of the prestack seismic data, considering that this optimization problem computationally very expensive.

In the first works, to make feasible the solution, the optimization problem of 3D CRS stack was usually split into several steps, each one searching for a subset of parameters. In Mullër (2003) the optimization problem of the 3D CRS stack was divided into three steps using the simplifications of the CRS traveltime approximation for common-midpoint (CMP) and zero-offset (ZO) configurations as a simplification to the optimization process. In the first step, called hyperbolic CMP search, three parameters related to wavefront curvatures of the NIP wave are determined. The second step is a two-parametric ZO search for the azimuth and dip angles of the central ray. In the third step, called hyperbolic ZO search, the three parameters related to wavefront curvatures of the Normal wave are determined. The grid search method is used for determining the stacking parameters in all three steps. At each point of grid, built up with a set of predefined parameters values, the objective function is evaluated and those parameters that produce the maximum value of coherence are selected. Usually, this approach is computationally very expensive because it uses a dense grid to ensure the determination of parameters of global maximum. Besides, the error is accumulated systematically, which can degrade the accuracy of the CRS stacking parameters and the quality of ZO stacked image. A detailed explanation of this optimization strategy, called pragmatic approach is also given in Bergler (2004).

In order to overcome the limitations of the pragmatic strategy, it is necessary to simultaneously determine all CRS parameters, but finding an effective global optimization strategy is a great research challenge. In Bonomi et al., (2009) the eight stacking parameters are determined simultaneously applying as a global optimization algorithm the conjugate-direction algorithm based on iterative line-search with an efficient rule for control of the step-size. They obtained an improved stacked image in comparison with the result of the multi-step approach. In Xie and Gajewski (2016) a simultaneous search of the 3D CRS parameters is performed by applying the an evolutionary-based Nelder-Mead algorithm, that combines the classical global optimization genetic algorithm to search for the initial solution and the local optimization downhill simplex or flexible polyhedron algorithm for the final refinement of all CRS parameters.

In this work, we present the application of the global optimization algorithm Very Fast Simulated Annealing (VFSA), to search simultaneously for the eight parameters of the 3D CRS stack method. In order to reduce the computational cost we also apply VFSA algorithm to search for simultaneously the five parameters of the 3D common-diffraction-surface (CDS) stack operator. We present a comparative study about the speed of convergence and effectiveness of VFSA algorithm in searching eight and five parameters. The performance of the VFSA is also investigated applying the CRS and CDS stacking methods to real land 3D dataset from Potiguar Basin, Brazil.

CRS and CDS traveltime approximations

The ZO 3D CRS stack method is based on the second-order hyperbolic reflection traveltime approximation for paraxial rays in the vicinity of a normal incidence central ray. Following the notation in Bergler (2004), the simplified form of the 3D CRS traveltime can be written as

$$t_{\mathrm{CRS}}^2(\Delta\mathbf{m},\mathbf{h}) = \left(t_0 + 2\mathbf{p}_0\cdot\Delta\mathbf{m}\right)^2 + \mathbf{h}^{\mathrm{T}}\,\mathbf{M}\,\mathbf{h} + \Delta\mathbf{m}^{\mathrm{T}}\,\mathbf{N}\,\Delta\mathbf{m} \quad (1)$$

where $\Delta\mathbf{m} = \mathbf{m} - \mathbf{m_0}$ denotes the displacement vector between the midpoint of the central ray, $\mathbf{m_0}$, and the midpoint of the paraxial ray, $\mathbf{m}$. The vector $\mathbf{h}$ is the half-offset coordinate between source-receiver positions of the paraxial ray. The two-component vector $\mathbf{p_0} = (p_{0,x}\,, p_{o,y})$ denotes the slowness vector projection of the ZO central ray onto the measurement surface at the emergence point and t_0 denotes the two-way traveltime along the central ray. The two symmetric 2 x 2 matrices $\mathbf{M}$ and $\mathbf{N}$ are given by

$$\mathbf{M} = \begin{pmatrix} m_{00} & m_{01} \\ m_{01} & m_{11} \end{pmatrix} = \frac{2t_0}{v_0}\mathbf{R}\,\widetilde{\mathbf{K}}_{\mathbf{NIP}}\,\mathbf{R}^{\mathrm{T}} \quad (2)$$

$$\mathbf{N} = \begin{pmatrix} n_{00} & n_{01} \\ n_{01} & n_{11} \end{pmatrix} = \frac{2t_0}{v_0}\mathbf{R}\,\widetilde{\mathbf{K}}_{\mathbf{N}}\,\mathbf{R}^{\mathrm{T}} \quad (3)$$

The matrices $\widetilde{\mathbf{K}}_{\mathbf{NIP}}$ and $\widetilde{\mathbf{K}}_{\mathbf{N}}$ are the curvature matrices of the normal-incidence-point (NIP) wave and normal wave, respectively (Hubral, 1983), expressed with respect to the ray-centered system defined by the transformation matrix **R**. The parameter $\mathbf{p_0}$ provides information about the local dip of the reflector at the NIP, $\widetilde{\mathbf{K}}_{\mathbf{NIP}}$ provides the depth location of the reflector at the NIP and $\widetilde{\mathbf{K}}_{\mathbf{N}}$ provides the local curvature of the reflector at the NIP. Then, the CRS traveltime (1) depends on eight unknown parameters $(\mathbf{p_0}\,, \mathbf{M}, \mathbf{N})$.

Considering the NIP point on the reflector surface as a scatter point or diffractor, the traveltime approximation (1) can be simplified by applying the diffraction condition, $\mathbf{N} = \mathbf{M}$, then, the equation (1) reduces to

$$t_{\mathrm{CDS}}^2(\Delta\mathbf{m},\mathbf{h}) = \left(t_0 + 2\mathbf{p}_0\cdot\Delta\mathbf{m}\right)^2 + \mathbf{h}^{\mathrm{T}}\,\mathbf{M}\,\mathbf{h} + \Delta\mathbf{m}^{\mathrm{T}}\,\mathbf{M}\,\Delta\mathbf{m} \quad (4)$$

This traveltime is the so-called the 3D Common-Diffraction-Surface (CDS) stacking operator and it depends only on five parameters $(\mathbf{p_0}\,, \mathbf{M})$.

The equation (1), even for an inhomogeneous media above the reflector, approximates the true reflection traveltimes in the vicinity of a ZO sample point $P_0 = (m_{0,x}, m_{0,y}, t_0)$ and the amplitudes along the stacking operators are summed up to simulate the ZO amplitude at P_0. Although the CDS operator (4) best fit diffraction events, it can also be used to fit reflection events within a small aperture in the midpoint coordinate.

In order to simulate a ZO stacked volume from 3D multi-coverage seismic data by using the 3D CRS and CDS stacking operators, it is necessary to find, for each time sample of the ZO volume to be simulated, the CRS parameters that yields the stacking operator fitting best to any reflection or diffraction events in the multi-coverage prestack data.

Therefore, the main task of the CRS or CDS method is to solve the optimization problem to provide the CRS stacking parameters accurately and efficiently. In this work, we apply the global optimization algorithm VFSA.

Cost function of the CRS method

For any application of the stacking operators (1) and (4), it is necessary to determine the CRS parameters from multi-coverage prestack data, by means of global optimization algorithms based on coherence measurement of the prestack seismic signal. The eight parameters that define the CRS operator are: $\mathbf{p_0}$, $\mathbf{M}$ and $\mathbf{N}$. For the CDS and CRS operators are required only the parameters $\mathbf{p_0}$ and $\mathbf{M}$.

As cost or objective function in the optimization problem of the CRS type methods we used the coherence measure semblance (Neidell and Taner, 1971):

$$S(\mathbf{m_0}, t_0) = \frac{1}{L}\frac{\sum_t\left(\sum_{i=1}^{L} U_{i,t(i)}\right)^{\mathbf{2}}}{\sum_t\sum_{i=1}^{L} U_{i,t(i)}^2}\,, \quad (\mathbf{6})$$

where $U_{i,t(i)}$ represents the amplitude of the seismic trace indexed by $i = 1, \ldots, L$, being L the number of seismic traces for coherency analysis. In the time window the amplitudes are located according to the CRS or CDS traveltime approximations, i.e., $t(i) = t_{CRS}(\mathbf{p_0}, \mathbf{M}, \mathbf{N}, \mathbf{\Delta m}, \mathbf{h})$ or $t(i) = t_{CDS}(\mathbf{p_0}, \mathbf{M}, \mathbf{\Delta m}, \mathbf{h})$.

The coherence semblance (6) yields multimodal functions for the CRS or CDS operators, but, usually, it has one prominent minimum for a strong reflection or diffraction event. However, it may have some prominent minima, when is related to events with conflicting dips. In this work, the proposed optimization strategies are concerned only to find the global minimum, that is, to find only one optimum solution for each time sample point of the ZO trace. To solve the optimization problem of CRS and CDS operators, we applied the VFSA global optimization algorithm which shown to be appropriate to find a global optimum solution of multidimensional multimodal objective functions.

Global optimization of the CRS parameters

The Simulated Annealing optimization is a stochastic search method based on the imitation of nature skills. It mimics the thermodynamic process of slow cooling (annealing) of molten metals to attain the lowest free energy state (Kirkpatrick et al., 1983). It can be applied to minimize a multidimensional cost function, but it is slow in reaching the optimum solution. The VFSA algorithm introduced by Ingber (1989) is an improved version of the Simulated Annealing algorithm, where convergence to the optimum solution is very fast. The annealing schedule for VFSA algorithm is given by: $T_i(k) = T_{0_i}\exp(-c_i k^{1/N})$, were *i* denotes *i*th variable of cost function and *N* the number of variables or dimension of the search-space.

Table 1 – CRS and CDS parameters obtained by global optimization VFSA algorithm

	Coher	Azimuth	Dip	m_{00}	m_{01}	m_{11}	n_{00}	n_{01}	n_{11}
CRS	0.090	101.20	-9.43	3.188e-07	4.437e-08	2.954e-07	-2.493e-07	-5.609e-08	-2.872e-07
CDS	0.081	104.01	-9.18	3.189e-07	5.406e-08	2.859e-07			

We use one initial temperature, T_{0_i}, and one constant decay value or cooling rate factor, c_i. The parameter k is the number of trial moves or attempts that control the annealing time steps. As stopping criterion is used the error tolerance and the algorithm also can stop the process when a maximum number of cost function evaluations is reached. A description of the VFSA algorithm applied to the solution of the optimization problems of the 2D ZO CRS and 2D CO CRS stacking methods can be found in Garabito et al., (2012 and 2016).

An appropriate value of T_{0_i} allow the VFSA algorithm to explore the entire cost function and escape from local minima by the uphill moves. The value of T_{0_i} depends on the scaling of the cost function and there are some formulas to estimate it. The cooling rate factor, c_i, is the parameter that has the greatest influence on the performance of the algorithm because it controls the fast or slow convergence, i.e., for larger values of c_i the decay of temperature is very fast and consequently the VFSA algorithm could get stuck in a local minimum.

For effective application of the VFSA algorithm, it is necessary to conduct a suitable selection of their control parameters. In this work, the selection of the control parameters and the performance studies for VFSA were done through the several convergence runs for some time sample points chosen on different reflection events of a 3D real data. Here, we show the results for only one ZO time sample point ($t_0 = 1.04s$) located on a reflection event with low coherence. Thus, the values for control parameters of VFSA estimated through several convergence runs are: $T_{0i} = 0.4$, $c_i = 0.4$a and $k = 50$ to search for 8 and 5 CRS parameters.

Using this control parameters and for a the ZO sample ($t_0 = 1.04s$), in Figures 1 and 2 we show the performance tests of the VFSA algorithm to search simultaneously eight parameters equation (1) and five parameters of the equation (4). Each Figure show 10 convergence curves of single runs. Figure 1 shows the convergence to the global minimum after 1700 evaluations of the eight dimensional CRS cost function. Figure 2 shows the convergence to the global minimum after 800 evaluations of the 5 dimensional CDS cost function. In Table 1 are shown the average of the optimized CRS parameters using the two stacking operators.

The azimuth and dip angles and the elements of the diagonal of the matrix $\mathbf{M}$ have very close values for the CRS and CDS operators; however, the element m_{01} has different values for both operators. The differences of the values of m_{01}, as well as the different values of coherence shown in Table 1, are due to the sensitivity of the size of the CDS operator, that is, different sizes of this operator cause changes in the values of the parameters. Usually the size of the aperture of the CDS operator must be small compared with the size of the CRS operator.

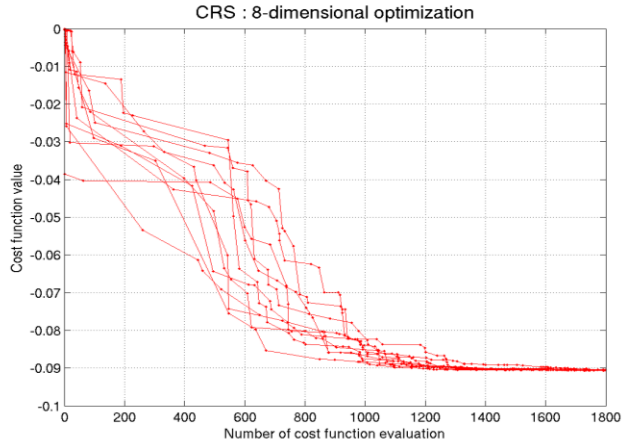

***Figure 1** – Convergence plot of the VFSA algorithm for simultaneous search of 8 parameters of the CRS operator presented in equation (1).*

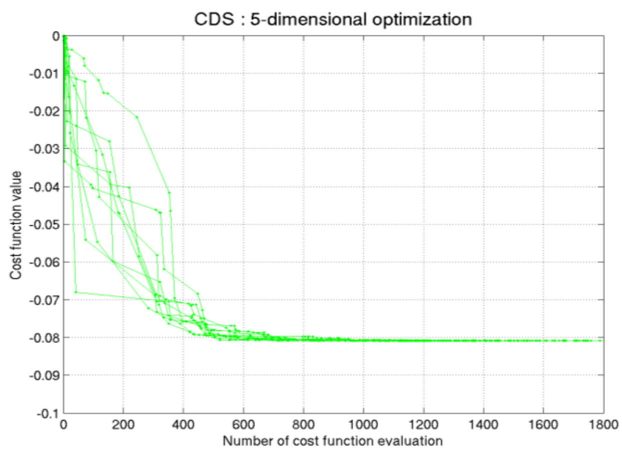

***Figure 2** – Convergence plot of the VFSA algorithm for simultaneous search of 5 parameters of the CDS operator presented in equation (4).*

Applications to real land data

We apply the CRS and CDS stacking methods to real 3D land dataset acquired in Potiguar basin, northeast Brazil, and with the permission of Sonangol Hidrocarbonetos Brasil (SHB) and Petrobras companies, the preliminary results will be shown here. The complete data processing with the proposed methods is still in progress.

This land dataset has been acquired with orthogonal geometry, producing a good azimuthal distribution of the data. The receivers lay-out had 12 parallel lines at 100m interval and 50m interval receiver stations. The shots are move orthogonal to receiver lines; the interval of shot lines is 150m, and the interval between shots is 110m. The nominal fold is 120, and the processing grid is 25m along cross-line and 50m in-line.

The processing flow applied to the data is: 1) Field Static corrections, 2) Geometrical Spreading correction, 3) Coherent noise attenuation, 4) Surface consistent deconvolution, 5) Spectral whitening, 6) velocity analysis, 7) NMO correction 7) Residual statics application, 8) update of velocity model, 9) NMO correction, 10) mute analysis, 11) inverse NMO correction.

The output data from this processing flow was input to CRS and CDS stack methods.

In order to compare with the results of the two stacking methods (CDS and CRS), we also present the result of the standard processing, which is a post-stack migration of an in-line (Figure 3).

The result in Figure 3 was obtained by applying 3D standard CMP stack and a 2D poststack time migration to one single in-line. As expected, this result has a low quality, where the reflection events are not clearly defined mainly in the left and upper parts of the section.

In Figures 4 and 5 are shown, respectively, the results of the 3D CDS and CRS stacking methods. In these results, for a fair comparison with the standard result, we also apply a 2D poststack time migration. The CDS stack result (Figure 4) shows a good improvement in quality for almost the entire section. In Figure 5 we present the result of the 3D CRS stack method and as expected the signal-to-noise ratio was strongly increased compared to the CDS stack and the standard CMP stack. The CRS stack result shows a clearer image, with good continuity of reflection events in whole section.

Discussion

The CDS stack method requires a small aperture size to fit the prestack reflection events, consequently, the number of traces involved in stacking process is lower than in the CRS method. For this reason, the CDS stack result has relatively low quality compared to the CRS stack. On the other hand, the low quality in the upper part of the CDS result is also influenced by the scale of the grid, which is relatively large in the in-line direction (50m). However, as shown in Figure 2, the convergence of the optimization process using the CDS operator is faster and therefore the computational cost to apply the CDS stack method is lower. The CRS stack method uses larger number of traces to simulate a ZO stacked trace. As shown in Figure 1, the global optimization of the eight CRS parameters requires a large number of cost function evaluations to converge to the global minima, so the computational cost is expensive to obtain the entire stacked volume of a 3D data.

For example, the CPU time to obtain only the in-line shown in Figures 4 and 5 are 46 min and 237 min, respectively. The codes are parallelized and to obtain these results we use 50 cores of a shared memory machine.

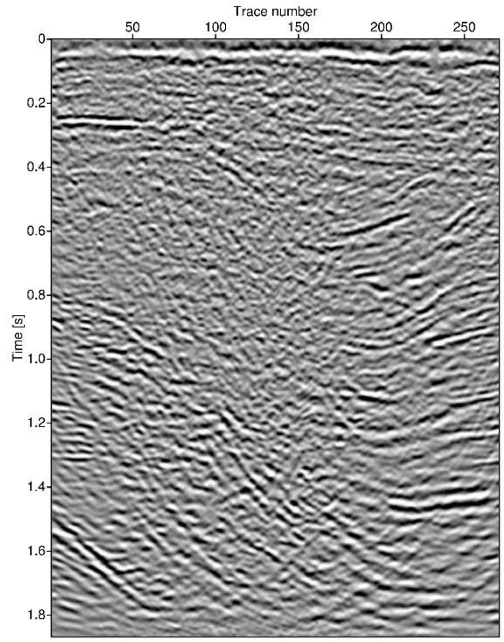

Figure 3 *– Time migrated in-line produced by standard CMP stack method and post-stack time migration.*

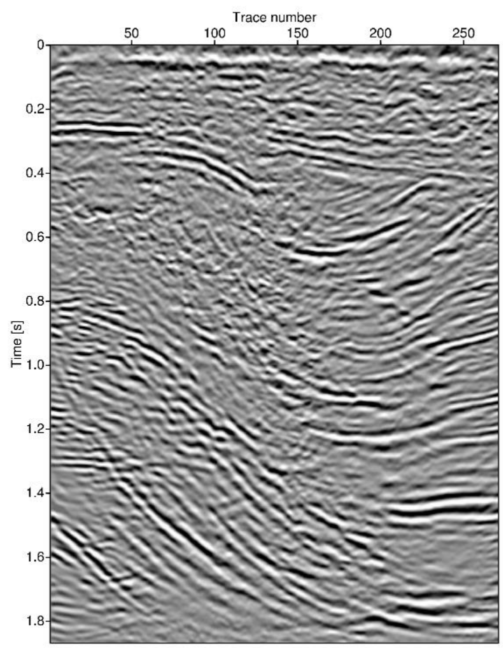

Figure 4 *– Time migrated in-line produced by 3D CDS stack method and post-stack time migration.*

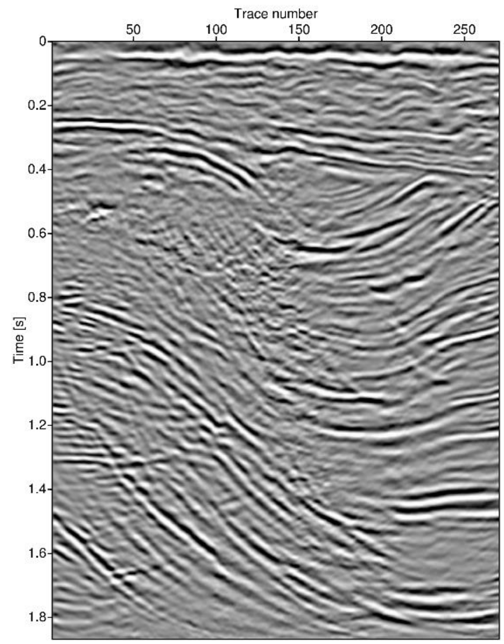

Figure 5 *– Time migrated in-line produced by 3D CRS stack method and post-stack time migration.*

Conclusions

We present a global optimization solution applying the VFSA algorithm to search simultaneously the five and eight parameters of the CDS and CRS operators. The convergence plots are helpful to show the performance of the VFSA algorithm and the maximum number of cost function evaluations to reach the optimal solution.

The CDS stack result show significant improvements in image quality and resolution that the standard CMP stack result. The CRS stack method gives the best results, with high quality and clearer image of the reflections events than the CDS stack and CMP stack methods. The CDS method is fast and computationally inexpensive, but it can provide better results for dataset with small and equal processing grid in in-line and cross-line directions.

As additional results of the CRS method provides eight accurate stacking parameters (or kinematic attributes), they can be applied with confidence to prestack data regularization, velocity model determination and others.

Acknowledgments

We thank to Sonangol Hidrocarbonetos Brasil (SHB) and Petrobras petroleum companies for the permission to present in this work the results of the 3D dataset of Potiguar basin, Brazil.

References

Bonomi, E., Cristini, A., Theis, D., and Marchetti, P. 2009, 3D CRS analysis: a data-driven optimization for the simultaneous estimate of the eight parameters: SEG Technical Program, Expanded, Abstracts, 3284–3291.

Borrini, D., Cristini, A., Follino, P., Marchetti, P., Zamboni, E., 2005, 3D CRS processing: a better use of Pre-stack data. Expanded Abstract, SEG Annual Meeting, Houston, Texas.

Bergler, S., Hubral, P., Marchetti, P., Crisitni, A., and Cardone, G., 2002, 3D common-reflection-surface stack and kinematic wavefield attributes: The Leading Edge, **21**, 1010–1015.

Bergler, S., 2004, On the determination and use of kinematic wavefield attributes for 3D seismic imaging. PhD thesis, Geophysical Institute, University of Karlsruhe. Logos Verlag Berlin.

Cristini, A., Cardone, G., and Marchetti, P., 2002, 3D Zero-Offset Common Reflection Surface Stack for Land Data: Real Data Example, 64th EAGE Conference & Exibition, Expanded Abstracts B-15, Florence, Italy.

Garabito, G., Stoffa, P.L., Lucena, L.S., Cruz, J.C.R., 2012. Part I - CRS stack: Global optimization of the 2D CRS-attributes. Journal Applied Geophysics 85, 92-101.

Garabito, G., Cruz, J. C. R. and Söllner, W., 2016, Finite-offset common reflection surface stack using global optimization for parameter estimation: a land data example. Geophysical Prospecting. doi:10.1111/1365-2478.12472

Ingber, L., 1989. Very fast simulated re-annealing. Mathematical and Computer Modelling 12 (9), 967–973.

Kirkpatrick, S., Gelatt, C., Vecchi, M., 1983. Optimization by simulated annealing. Science 220, 671–680.

Müller, N. A., 2003, The 3D Common-Reflection-Surface stack: theory and application: Master thesis (*Diplomarbeit*), Geophysical Institute, University of Karlsruhe.

Müller, N. A., 2009, Treatment of conflicting dips in the 3D common-reflection-surface stack. Geophysical Prospecting, 57, 981–995

Neidell, N., Taner, M., 1971. Semblance and other coherency measures for multichannel data. Geophysics 36, 482–497.

Xie, Y. and Gajewski, D., 2016, Simultaneous estimation of the 3D CRS attributes by an evolutionary-based Nelder Mead algorithm: SEG Technical Program, Expanded Abstracts, 4326-4330.